



## Journal of Materials Chemistry C

ARTICLE

### Electronic Supplementary Information

## Multiplex Plasmonic Nanopillar Arrays Encoded with Molecular Information for Anti-counterfeiting Applications

Y. Liu,<sup>a</sup> Y. H. Lee,<sup>a</sup> Q. Zhang,<sup>a</sup> Y. Cui<sup>a</sup> and X. Y. Ling<sup>a\*</sup>

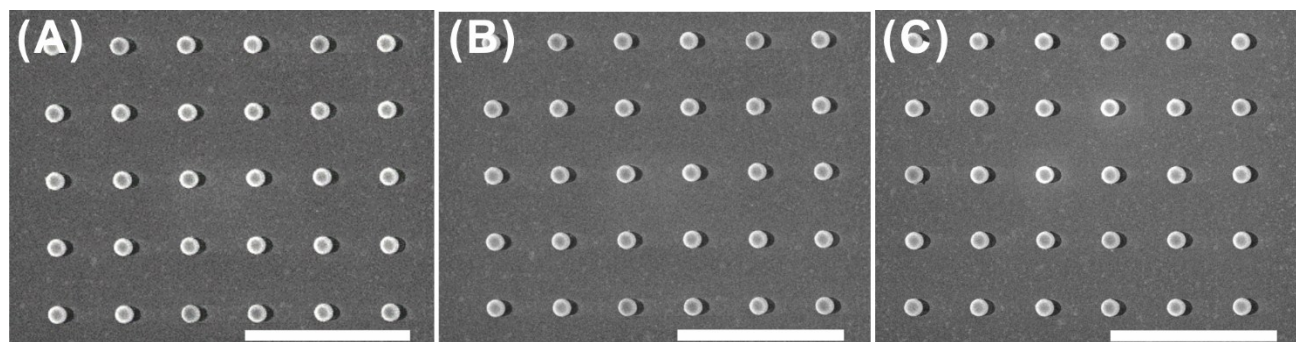


**Figure S1.** Comparison on morphologies of photoresist nanopillar and dye-encapsulated nanopillars. SEM images of (A) photoresist nanopillar, (B) R6G-encapsulated nanopillars, and (C) EY-encapsulated nanopillars, respectively. Scale bar represents 5  $\mu\text{m}$ .

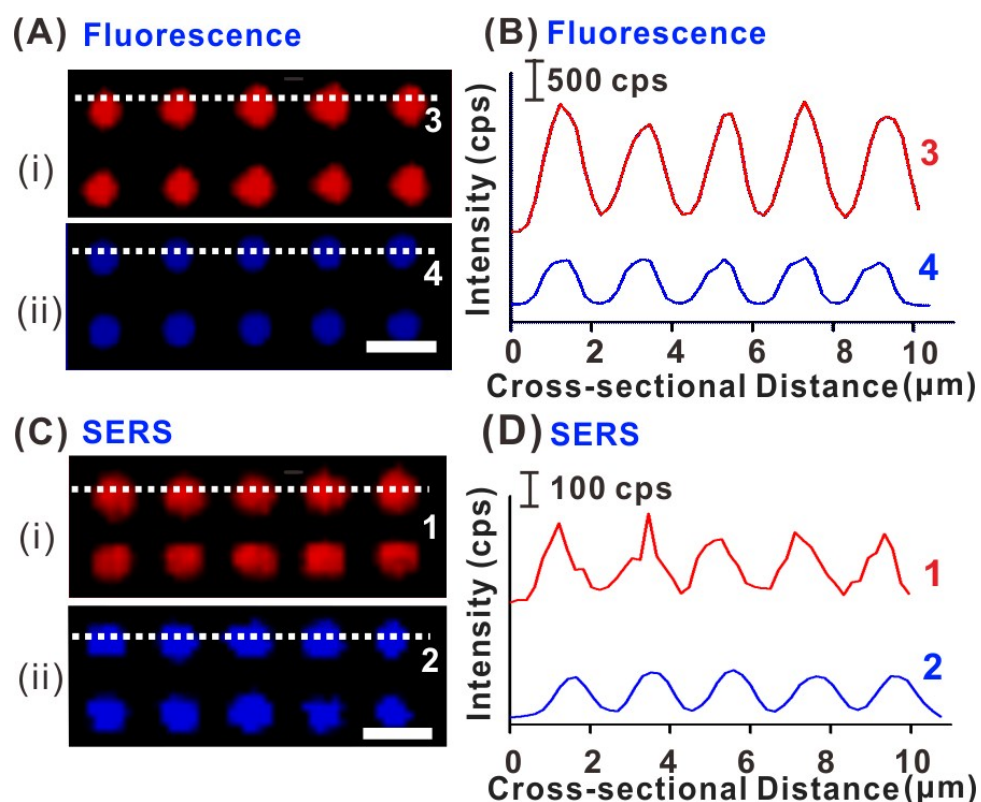


**Figure S2.** Homogeneity of SERS and fluorescence signals on dye-encapsulated nanopillars. (A) Fluorescence images taken from the (i) R6G- and (ii) EY-encapsulated nanopillars at 560 (for R6G) and 630 nm (for EY). (B) Cross-sectional fluorescence intensity profile along lines 3 and 4, labeled in (A). (C) SERS images of (i) R6G- and (ii) EY-encapsulated nanopillars created by selecting their respective vibrational bands at 622 (for R6G) and 1639  $\text{cm}^{-1}$  (for EY). (D) Cross-sectional SERS intensity profile along lines 1 and 2 in (C). Scale bar represents 2  $\mu\text{m}$ .

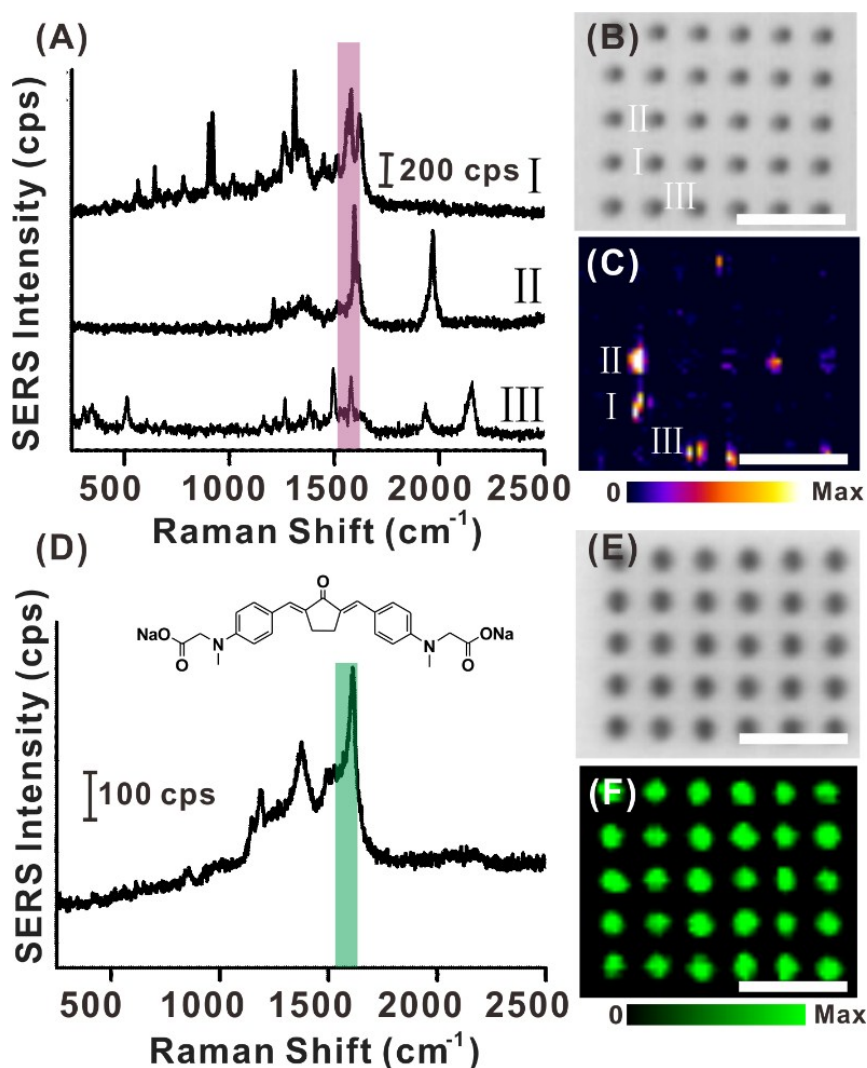


**Figure S3.** SERS spectra comparison between commercial photoresist IPL-780 and our photoresist. (A) SERS spectra of Ag-coated pure IPL structures taken at points I, II, and III. (B) bright-field microscopic and (C) SERS images of Ag-coated pure IPL-780 arrays using the 1607 cm<sup>-1</sup> vibrational peak. (D) SERS spectra taken from Ag-coated pure photoresist arrays using our photoresist. (E) bright-field microscopic and (F) SERS images of Ag-coated pure photoresist arrays. The colors are assigned by relative intensity of the spectrum at 1607 cm<sup>-1</sup>. Scale bar represents 5 μm. Nanopillars produced by using the commercial photoresist IPL-780 create non-homogeneous and disordered SERS signals (A), because IPL-780 is composed of two ingredients as monomer and photo-initiate separately. Different polymerization extents generate various molecular structures, giving rise to the non-homogeneous SERS signals. Moreover, selecting at 1607 cm<sup>-1</sup> which is the common peak shown in all SERS spectra gives rise to non-uniform SERS images (A), thus IPL is not a suitable base material for SERS applications in our current system. On the other hand, SERS measurement on the nanopillar arrays fabricated by using our photoresist with a single component gives rise to clean SERS spectra with three main vibrational modes at 1180, 1370 and 1607 cm<sup>-1</sup> (D). Selecting at 1607 cm<sup>-1</sup> homogeneously illuminates the entire array in SERS images.

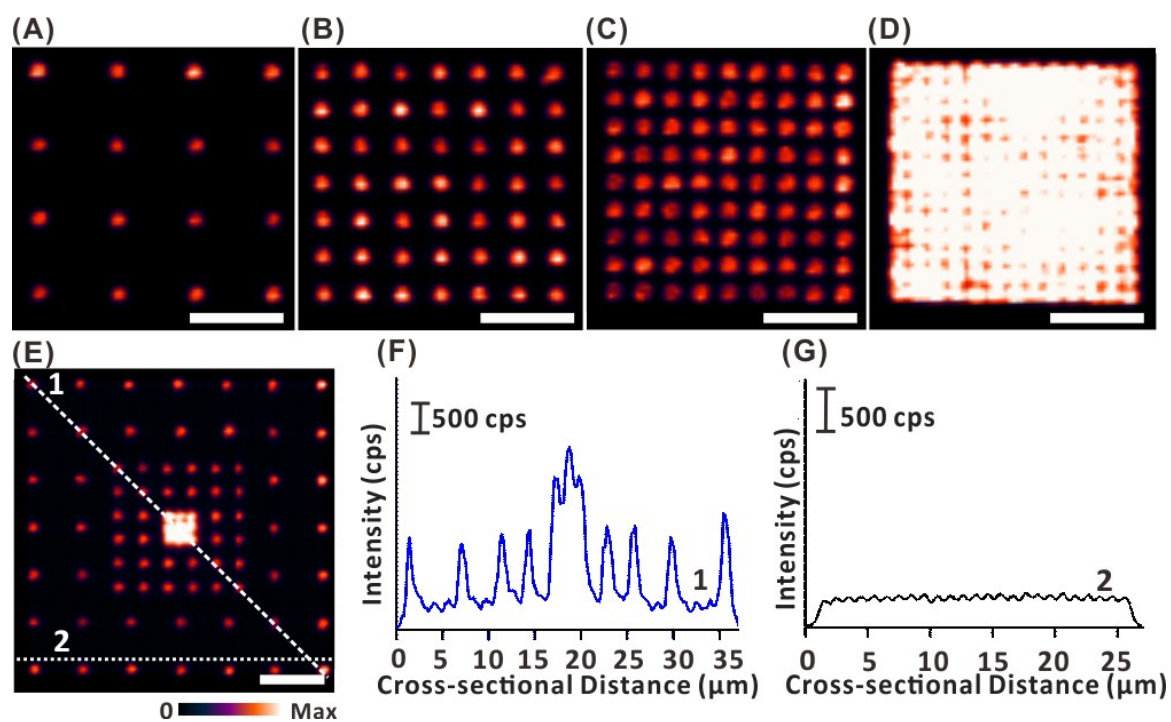


**Figure S4.** Fluorescence intensity grayscale images of the nanopillar array. (A-D) Fluorescence images of R6G-encapsulated nanopillars with different inter-pillar gaps. The distances between the pillars are (A) 3.5  $\mu\text{m}$ , (B) 1.5  $\mu\text{m}$ , (C) 1  $\mu\text{m}$  and (D) 0.5  $\mu\text{m}$ . (E) Fluorescence image and cross-sectional SERS intensity profile along (F) line 1 and (G) line 2 labeled in (E), respectively. Scale bar represents 5  $\mu\text{m}$ .

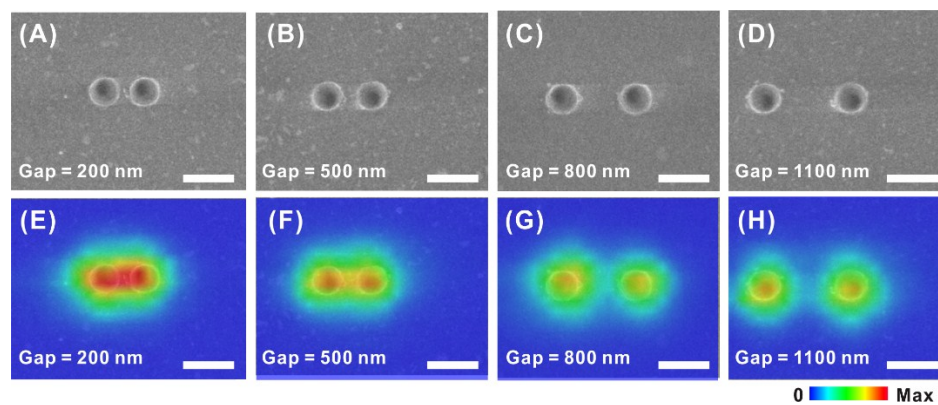


**Figure S5.** Influence of gap distance in the R6G-encapsulated nanopillar dimer. (A-D) SEM and (E-H) Overlapping SERS images of R6G with SEM images of Ag nanopillar dimers with inter-pillar gap distances of 200, 500, 800 and 1100 nm, respectively. The colors in SERS images are assigned by the vibrational signature of R6G at  $622\text{ cm}^{-1}$ . All scale bars represent  $1\ \mu\text{m}$ .

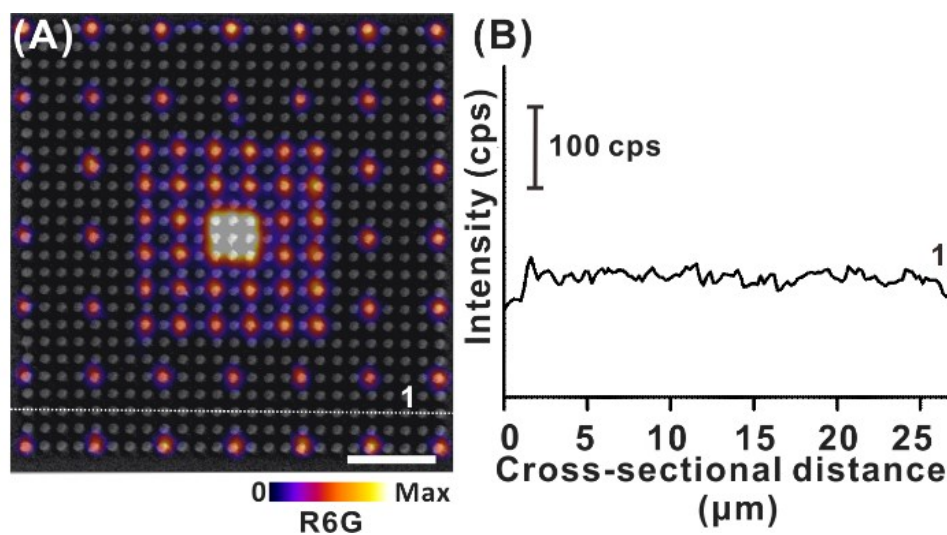


**Figure S6.** Intensity profile of the grayscale nanopillar array. (A) Overlaid SERS and SEM images. (B) Cross-sectional SERS intensity profile along line 1 in (A). Scale bar represents 5  $\mu\text{m}$ .

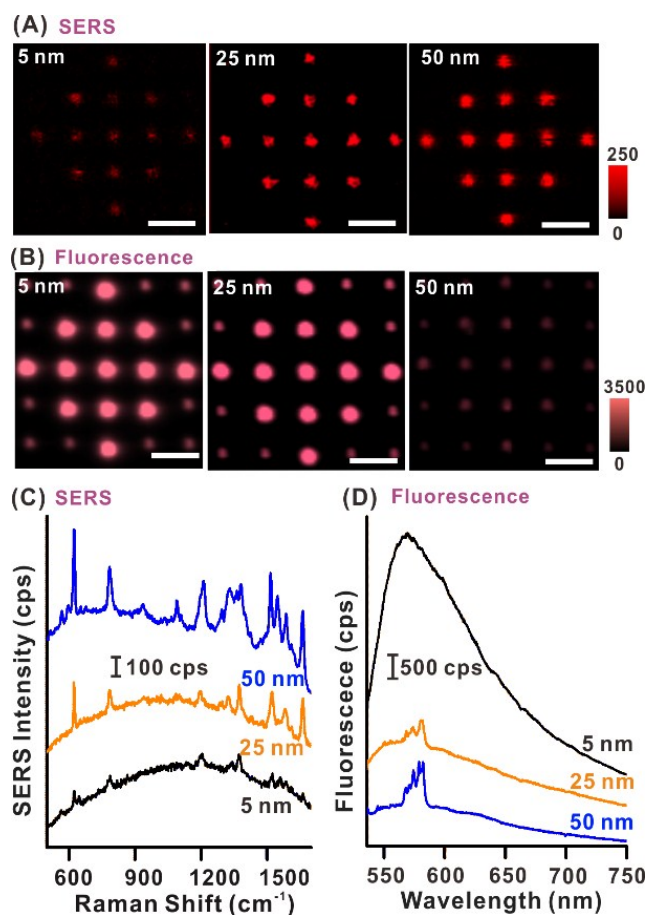


**Figure S7.** Influence of Ag thickness in the multiplex array. (A) SERS and (B) fluorescence images of R6G in the multiplex arrays which are deposited with 5 nm, 25 nm and 50 nm of Ag films, respectively, derived using the 622 cm<sup>-1</sup> mode for R6G. (C) SERS and (D) fluorescence spectra taken from R6G-encapsulated nanopillars in the multiplex arrays which are deposited with 5 nm, 25 nm and 50 nm of Ag films, respectively.

We deposit 25-nm thickness of Ag layer to give both strongly SERS-active and fluorescence-active nanopillars in the multiplex array. In the typical experiment, three multiplex arrays of nanopillars encapsulated with R6G and EY are fabricated by using the same protocol demonstrated in Figure 3A. Different thickness of Ag film are deposited on these multiplex arrays, increasing from 5 nm, 25 nm, to 50 nm. From SERS measurements of R6G on R6G-encapsulated nanopillars, we observe that the SERS signals of R6G increase with the thickness of Ag film (A and C). However, the fluorescent emissions are reduced when the thickness of Ag film is increased (B and D). Stronger SERS/fluorescence signals lead to a greater contrast between the nanopillars and the background in corresponding images, with more accurate information readouts. In our encoding platform, both SERS and fluorescence of the encapsulated dye molecules are encoded information which are supposed to be clearly read out. In the multiplex array deposited with 5-nm Ag, the fluorescence information is clearly read out but the SERS spectra/image can be hardly discerned. In the multiplex array coated with 50-nm Ag, the SERS spectra/image are resolved but the fluorescence is rather dim. Thus, we select 25 nm as the optimal thickness of Ag film to enable accurate decoding of both SERS and fluorescence information.



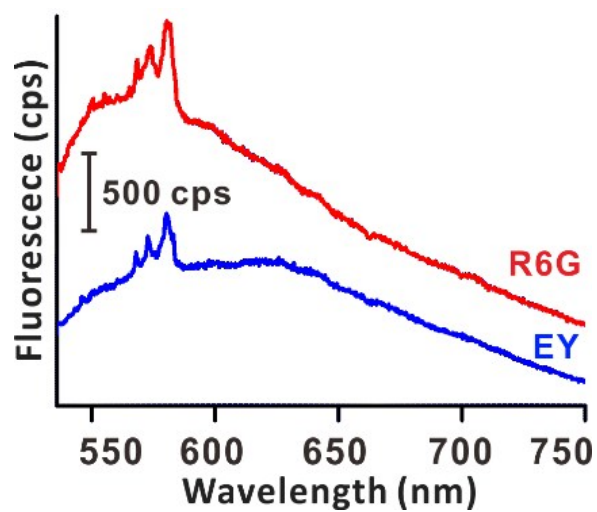


**Figure S8.** Fluorescence spectra taken from R6G- (red) and EY-encapsulated nanopillars (blue) in the multiplex nanopillar array, respectively.

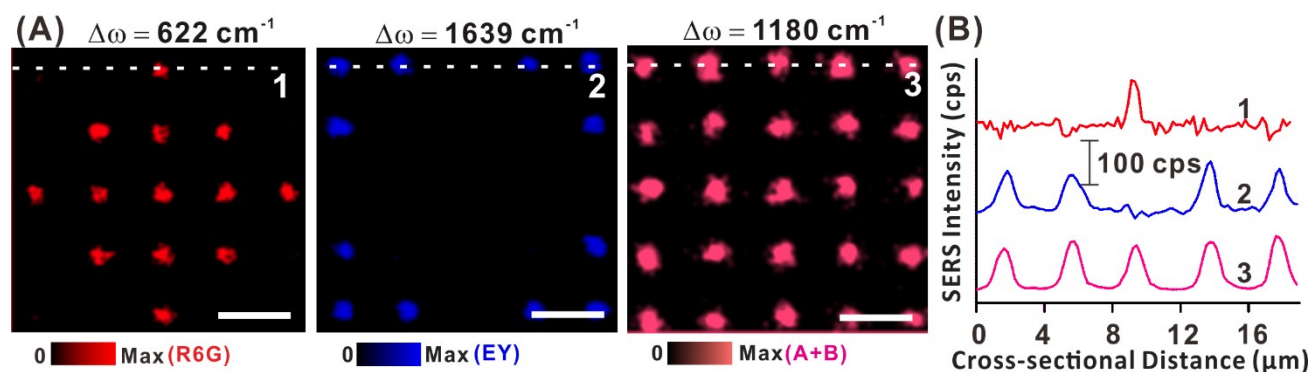


**Figure S9.** SERS taken from the multiplex nanopillar array. (A) Vibration-mode-selective SERS images created by selecting at band  $622 \text{ cm}^{-1}$  (red, for R6G),  $1639 \text{ cm}^{-1}$  (For EY) and  $1180 \text{ cm}^{-1}$ , respectively; (B) cross-sectional SERS intensity profiles at position 1-3, labeled in (A), respectively. All scale bars represent  $5 \mu\text{m}$ .

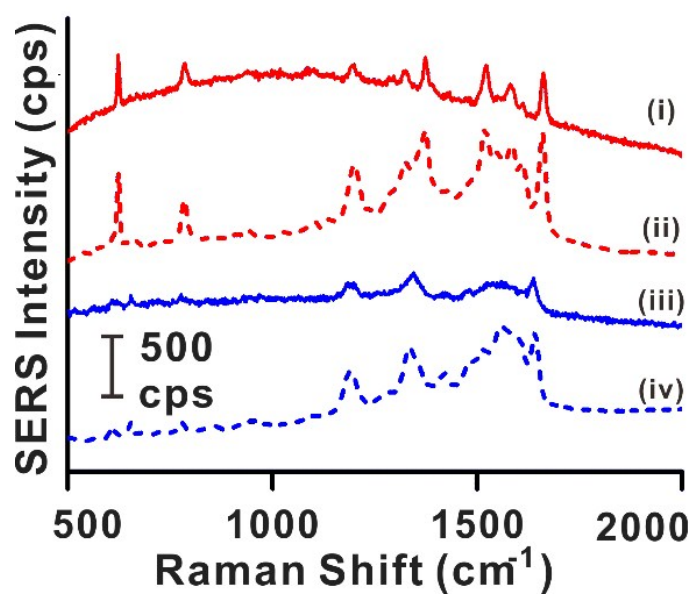


**Figure S10.** Comparison on SERS taken from the multiplex system and single-dye system. SERS taken from R6G-encapsulated nanopillars in (i) multiplex and (ii) single-dye system, respectively. SERS taken from EY-encapsulated nanopillars in (iii) multiplex and (iv) single-dye system, respectively.

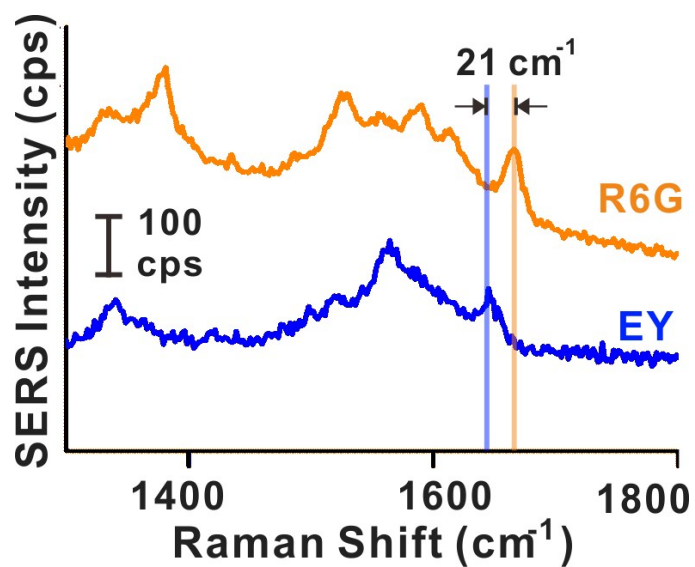


**Figure S11.** Zoom-in SERS taken from R6G- (orange) and EY-encapsulated nanopillars (blue) in ‘yin-yang’ pattern, respectively. The peak difference between 1639 cm<sup>-1</sup> for EY and 1660 cm<sup>-1</sup> for R6G is only 21 cm<sup>-1</sup>.

**Table 1.** Assignment of major vibrational peaks in SERS spectra of R6G-encapsulated nanopillars.

SERS band (cm <sup>-1</sup> )	Band assignment
622	xanthene ring/phenyl ring
785	in-plane deformation of the xanthene ring
1180	benzene ring stretches/symmetric CO <sub>2</sub> stretch
1321	C=C stretching vibration
1370	xanthene ring stretches/carboxylate stretches
1519	xanthene ring
1583	C=O stretching vibration/C=C symmetric stretching motion in phenyl group
1607	phenyl ring stretches
1660	C=C symmetric stretching mode in xanthene ring

**Table 2.** Assignment of major vibrational peaks in SERS spectra of EY-encapsulated nanopillars.

SERS band ( $\text{cm}^{-1}$ )	Band assignment
656	xanthene breathing/benzene ring breathing
779	xanthene ring stretches
1180	xanthene and benzene ring stretches/symmetric -COO stretch
1337	xanthene and benzene ring C-C stretches
1370	xanthene ring stretches/carboxylate group stretch
1420	xanthene ring stretches
1560	xanthene ring stretches
1607	benzene ring stretches
1639	xanthene ring stretches

z